Обзор ArXiv/astro-ph, 30 октября – 4 ноября 2019

От Сильченко О.К.

ArXiv: 1910.13457

On the Gas Content, Star Formation Efficiency, and Environmental Quenching of Massive Galaxies in Proto-Clusters at $z \approx 2.0 - 2.5$

J. A. Zavala,[1] C. M. Casey,[1] N. Scoville,[2] J. B. Champagne,[1] Y. Chiang,[3] H. Dannerbauer,[4,5] P. Drew,[1] H. Fu,[6] J. Spilker,[1] L. Spitler,[7] K. V. Tran,[8] E. Treister,[9] and S. Toft[10,11]

[1] *The University of Texas at Austin, 2515 Speedway Blvd Stop C1400, Austin, TX 78712, USA*
[2] *California Institute of Technology, MC 249-17, 1200 East California Boulevard, Pasadena, CA 91125, USA*
[3] *Department of Physics & Astronomy, Johns Hopkins University, 3400 N. Charles Street, Baltimore, MD 21218, USA*
[4] *Instituto de Astrofísica de Canarias (IAC), E-38205 La Laguna, Tenerife, Spain*
[5] *Universidad de La Laguna, Dpto. Astrofísica, E-38206 La Laguna, Tenerife, Spain*
[6] *Department of Physics & Astronomy, The University of Iowa, 203 Van Allen Hall, Iowa City, IA 52242, USA*
[7] *Department of Physics and Astronomy, Macquarie University, NSW 2109, Australia*
[8] *George P. and Cynthia W. Mitchell Institute for Fundamental Physics and Astronomy, Department of Physics & Astronomy, Texas A&M University, College Station, TX 77843, USA*
[9] *Pontificia Universidad Católica de Chile, Instituto de Astrofísica, Casilla 306, Santiago 22, Chile*
[10] *Cosmic Dawn Center (DAWN)*
[11] *Niels Bohr Institute, University of Copenhagen, Vibenshuset, Lyngbyvej 2, DK-2100 Copenhagen, Denmark*

(Accepted October 31, 2019)

ABSTRACT

We present ALMA Band 6 ($\nu = 233\,\mathrm{GHz}$, $\lambda = 1.3\,\mathrm{mm}$) continuum observations towards 68 'normal' star-forming galaxies within two Coma-like progenitor structures at $z = 2.10$ and 2.47, from which ISM masses are derived, providing the largest census of molecular gas mass in overdense environments at these redshifts. Our sample comprises galaxies with a stellar mass range of $1 \times 10^9\,M_\odot - 4 \times 10^{11}\,M_\odot$

Выборка: (прото)скопления на z>2 и 68 их членов

a massive cluster in formation, according to cosmological simulations (Chiang et al. 2013). This active formation phase is further support by the high number of extreme galaxies within the proto-clusters. The $z = 2.10$ structure contains 9 rare DSFGs and 4 AGNs, has a total star formation rate (SFR) of $\sim 5300\,M_{\odot}\,\mathrm{yr}^{-1}$, total stellar mass of $\sim 2 \times 10^{12}\,M_{\odot}$, a galaxy overdensy of $\delta_{\mathrm{gal}} \sim 8$, and an estimated total halo mass of $\sim 2 \times 10^{14}\,M_{\odot}$ (Spitler et al. 2012; Yuan et al. 2014; Hung et al. 2016; Casey 2016). Similarly, the $z = 2.47$ structure contains at least 7 rare DSFGs and 5 AGNs, implying an overdensity of $\delta_{\mathrm{gal}} \sim 10$, a total SFR of $\sim 4500\,M_{\odot}\,\mathrm{yr}^{-1}$, total stellar mass of $\sim 1 \times 10^{12}\,M_{\odot}$, and halo mass of $\sim 8 \times 10^{13}\,M_{\odot}$ (Casey et al. 2015; Casey 2016). This proto-cluster might indeed be embedded in a larger structure including several overdensities within a redshift range of $z = 2.42 - 2.51$ (Chiang et al. 2015; Diener et al. 2015; Lee et al. 2016; Wang et al. 2016; Cucciati et al. 2018; Gómez-Guijarro et al. 2019). Both structures are predicted to exceed $\gtrsim 1 \times 10^{15}\,M_{\odot}$ by $z = 0$. The sources targeted in this work are 'normal' star-forming galaxies with confirmed spectroscopic redshifts in these two structures. These rest-frame UV/optically selected systems are indeed expected to be more representative of the star-forming population than the extreme sources surveyed in previous studies, allowing for a detailed

Массивные галактики уже отклоняются вниз от MS и K-Sch

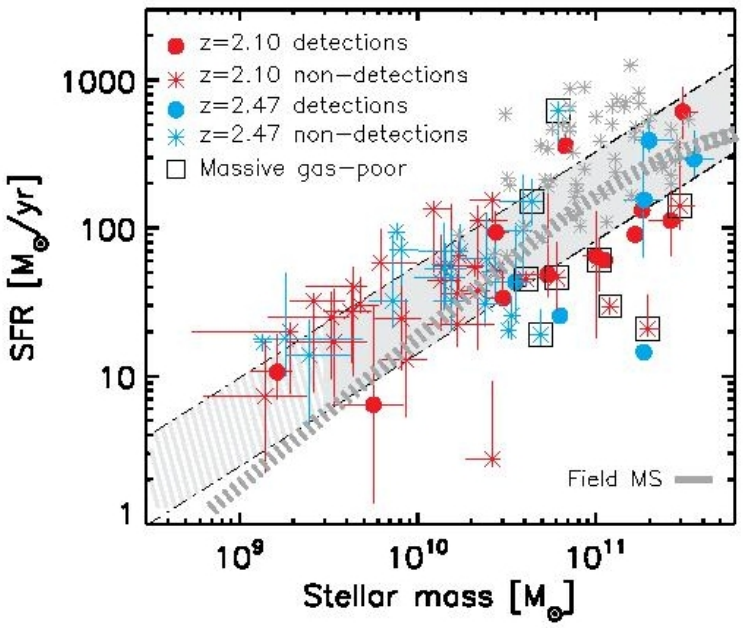

Figure 1. Distribution of our targets in the SFR-M_* plane in comparison with the star-forming main sequence. Sources detected with ALMA are represented by the blue and red solid circles while non-detections are identified with the blue and red asterisks. Blue symbols correspond to those galaxies in the $z = 2.47$ proto-cluster while red symbols denote members of the $z = 2.10$ structure. The adopted control sample drawn from Scoville et al. (2016) is shown as gray asterisks. Additionally, two different parametrization of the star-forming main sequence at the mean redshift of our sample are shown. The gray shaded area represents the relation derived by Speagle et al. (2014) and gray dashed line the one

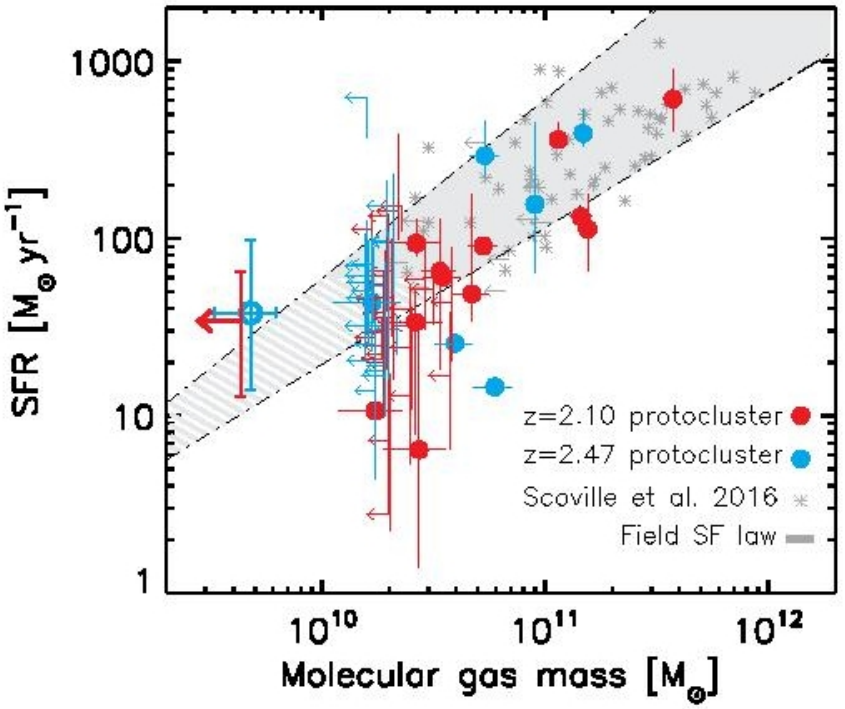

Figure 2. The SFR-$M_{\rm mol}$ relation as a proxy for the SFE. The $z = 2.10$ and 2.47 proto-clusters member galaxies detected by ALMA are represented by the red and blue filled circles, respectively, while the individual non-detections are plotted as 3σ upper limits (small red and blue left arrows). The 3.3σ detection from the stacking of the non-detected galaxies with SFRs $= 10 - 100$ in the $z = 2.47$ protocluster is illustrated by the large open blue circle, while the 3σ upper limit derived from the stacking of the analogous galaxies in the $z = 2.10$ proto-cluster is illustrated by the large red left

… и газа там мало

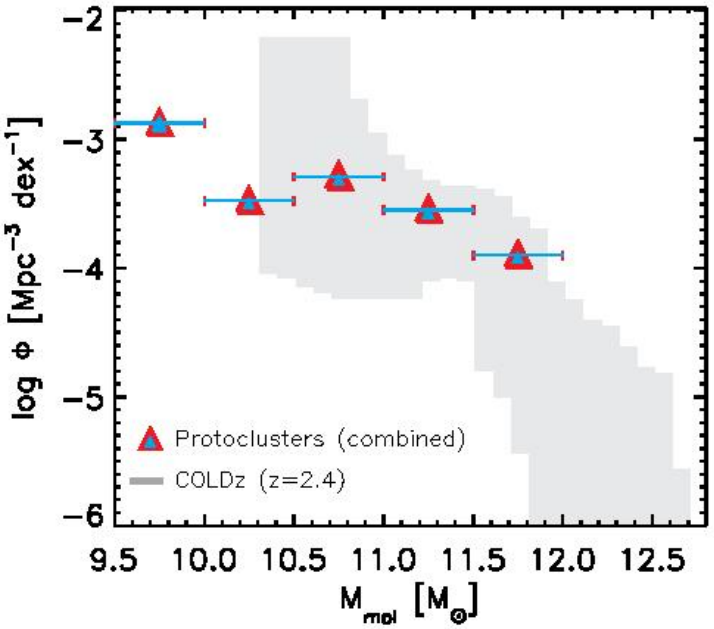

Figure 3. Comparison between the COLDz gas mass function derived from CO(1 − 0) observations at $z \approx 2.4$ (gray squares, Riechers et al. 2018) and the gas mass function derived from our ALMA follow-up of proto-cluster galaxies at similar redshifts (colored triangles). As described in the text, our measurements are formally lower limts since only a fraction of the proto-cluster members were observed. Therefore, it is likely that, after taken into account the incompleteness effects, the proto-clusters show an enhanced gas mass function (and hence gas volume density) compared to the field.

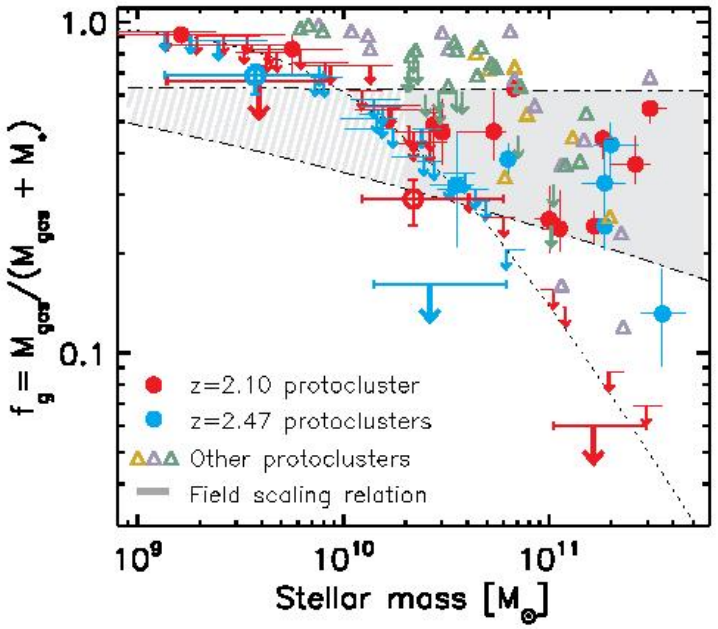

Figure 4. The molecular gas fraction of the proto-cluster members as a function of stellar mass (blue and red for the $z = 2.10$ and 2.47 structures, respectively), along with other measurements from the literature. Solid circles represent the ALMA detected galaxies while the small downward arrows are the respective upper limits for the individual non-detections. Large open circles and large downward arrows represent the results from the stacking of the non-detections of subsamples divided by stellar mass and redshift (see Table 3). The typical 3σ detection limit of our survey is illustrated by the dotted line. The derived gas mas fraction of most of the detected galaxies are in good agreement with

Еще и скопления-то нет, а quenching уже вовсю!

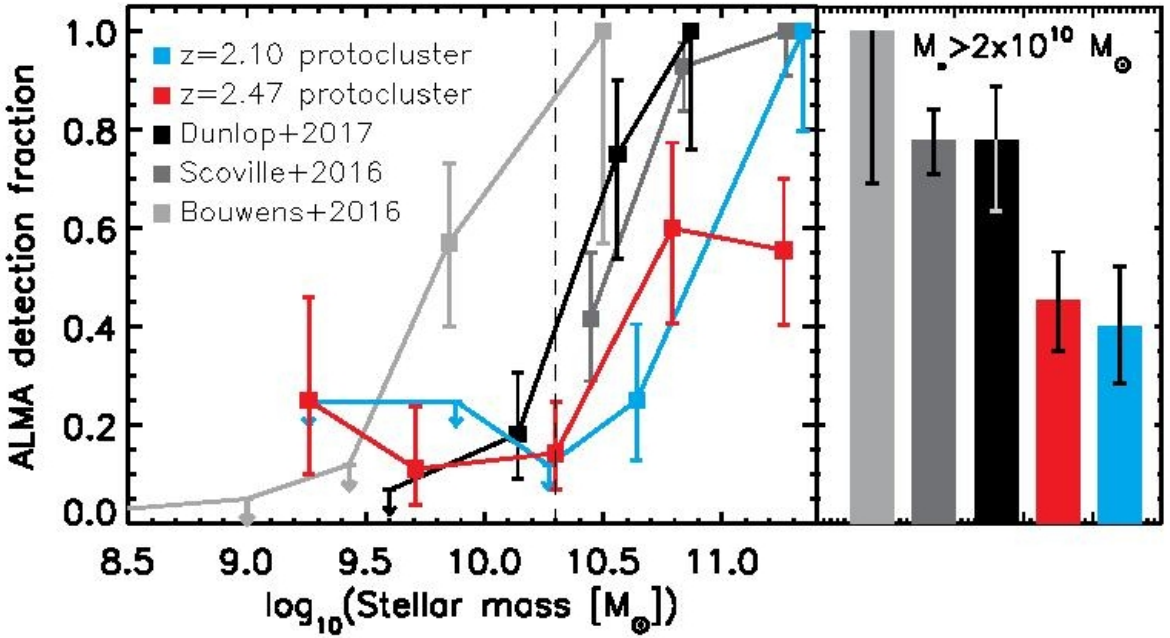

Figure 7. ALMA dust continuum detection fraction as a function of stellar mass for galaxies within $z \approx 2-3$. Previous ALMA blank-field observations (Bouwens et al. 2016; Dunlop et al. 2017) and follow-ups of field galaxies (Scoville et al. 2016) show a higher detection fraction than the one achieved towards the proto-cluster galaxies studied here (colored in red and blue), despite having similar depths. The difference is clearly evidenced by the detection fraction of the most massive galaxies ($M_\star > 2\times10^{10}\ M_\odot$), as shown in the right panel. This implies a higher fraction of quenched gas-poor galaxies in the proto-cluster structures than the one found in the field at the same cosmic epoch, suggesting that massive galaxies in dense environments undergo an accelerated evolution.

ArXiv: 1910.14017

Evidence for Non-smooth Quenching in Massive Galaxies at $z \sim 1$

Timothy Carleton[1⋆], Yicheng Guo[1], Hooshang Nayyeri[2], Michael Cooper[2], Gregory Rudnick[3], Katherine Whitaker[4, 5]

[1]*Department of Physics and Astronomy, 223 Physics Building, University of Missouri, Columbia, MO 65211, USA*
[2]*Center for Cosmology, Department of Physics and Astronomy, 4129 Reines Hall, University of California, Irvine, CA 92697, USA*
[3]*The University of Kansas, Department of Physics and Astronomy, Malott Room 1082, 1251 Wescoe Hall Drive, Lawrence, KS, 66045, USA*
[4]*Department of Physics, University of Connecticut, Storrs, CT 06269, USA*
[5]*Department of Astronomy, University of Massachusetts, 710 North Pleasant St, LGRT-524, Amherst, MA 01003, USA*

31 October 2019

ABSTRACT

We investigate a large sample of massive galaxies at $z \sim 1$ with combined *HST* broad-band and grism observations to constrain the star-formation histories of these systems as they transition from a star-forming state to quiescence. Among our sample of massive ($M_* > 10^{10}$ M$_\odot$) galaxies at $0.7 < z < 1.2$, dust-corrected Hα and UV star-formation indicators agree with a small dispersion (~ 0.2 dex) for galaxies on the main sequence, but diverge and exhibit substantial scatter (~ 0.7 dex) once they drop significantly below the star-forming main sequence. Significant Hα emission is present in galaxies with low dust-corrected UV SFR values as well as galaxies classified as quiescent using the *UVJ* diagram. We compare the observed Hα flux distribution to the expected distribution assuming bursty or smooth star-formation histories, and find that massive galaxies at $z \sim 1$ are most consistent with a quick, bursty quenching process. This suggests that mechanisms such as feedback, stochastic gas flows, and minor mergers continue to induce low-level bursty star formation in massive galaxies at moderate

Выборка

In our sample we select from the 1754 galaxies for which the 3D-HST catalogs contain a measurement of the Hα flux, have a stellar mass (M_*) above 10^{10} $M_\odot$, and are between z of 0.7 and 1.2. These limits are identified so that Hα is detectable well below the main sequence: the 3σ Hα detection limit taken from Momcheva et al. (2016) reaches 1.3 dex below the main sequence at $z = 1.2$ for point sources with no extinction. Additionally, we make the following cuts to our sample:

Много чего выкинули (AGN, низкий S/N...)

These cuts leave 780 galaxies overall, 417 of which have Hα emission above the 3σ level. All objects have at least one observation blue-ward of rest-frame 2800 Å, and 88% of objects have least one detection in that wavelength range, so the NUV luminosity is well constrained by observations.

- Данные: изображения в H и K на HST плюс БЕСЩЕЛЕВАЯ СПЕКТРОСКОПИЯ (объективная гризма) в области эмиссии H-alpha.

SFR по 2800 A и H-alpha

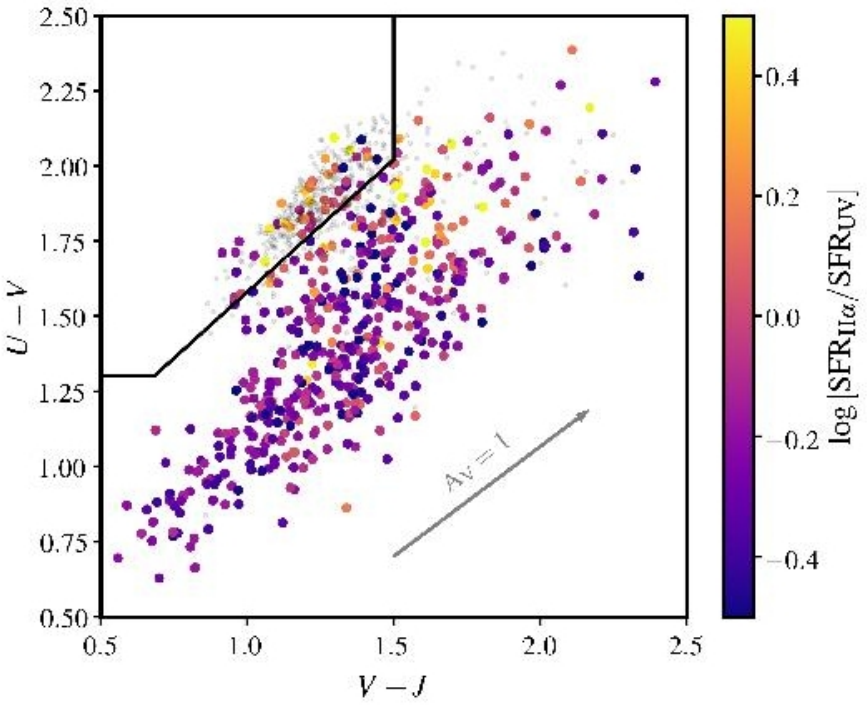

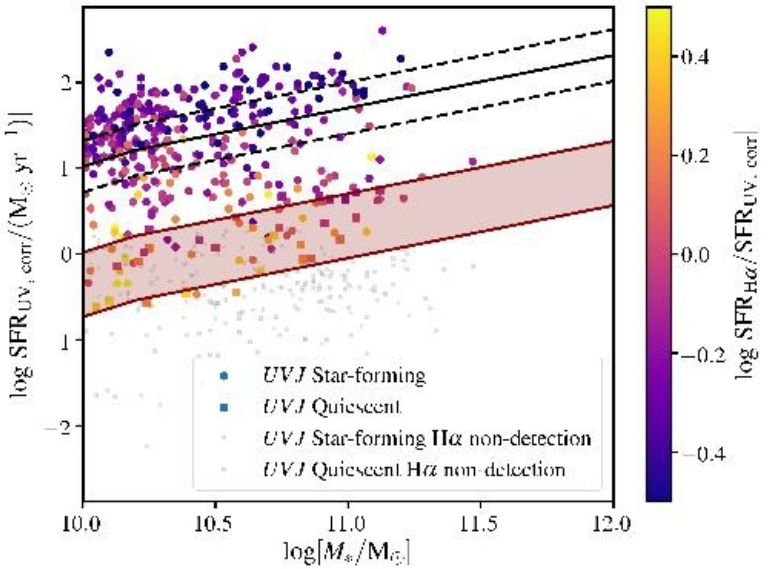

Figure 2. Our sample in SFR-M_* space. As in Figure 1, objects with Hα emission are color-coded by the ratio of their Hα and UV SFRs and grey points show objects with Hα non-detections. Points and squares show objects classified as *UVJ* star-forming and *UVJ*-quiescent respectively. The black solid and dashed lines show the main sequence from (Whitaker et al. 2014) and 0.3 dex scatter respectively. The red shaded region corresponds [illegible] below the main sequence, where we focus our in- [illegible] of UV-to-Hα SFR is uniform for objects on the [illegible] substantial variation for objects below the main sequence.

У всех H-alpha, НО делятся на starforming и passive

У тех, что падают вниз от MS, SF(H-alpha)>SF(UV)

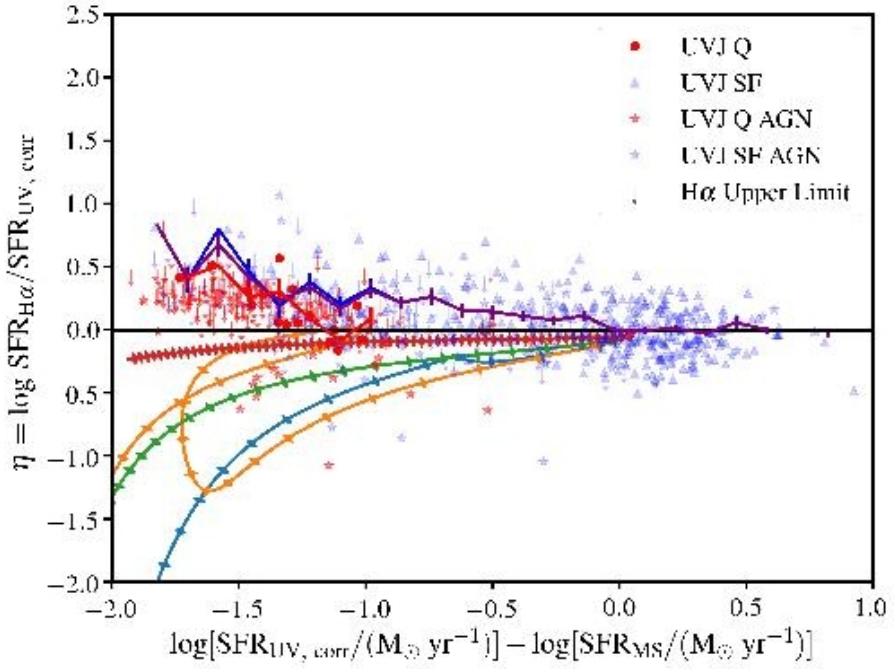

Figure 4. The relationship between η and ΔMS for galaxies in our sample. Galaxies are color-coded by whether they are classified as star-forming (blue) or quiescent (red) based on the *UVJ* diagram. The blue, red, and purple lines show the binned relationship between η and ΔMS for *UVJ*-star-forming, *UVJ*-quiescent, and all objects with Hα detections respectively. Arrows illustrate the 3σ limits of galaxies without a significant Hα detection. Although we do not include X-ray detected AGN in our primary sample, we show them here as stars to illustrate their distribution in this space. Star-forming galaxies with AGN actually have similar η values compared with galaxies without significant AGN, whereas quiescent galax-

HO...

2016). Although there remains uncertainty with regard to the specifics of AGB and post-AGB stellar evolution, models generally agree that evolved stars provide an ionizing flux of $\sim 10^{41}$ photons/s/$M_\odot$ (Cid Fernandes et al. 2011) independent of age. Assuming Case-B recombination and a temperature of 10,000 K, this corresponds to a Hα luminosity per stellar mass of 1.37×10^{29} erg s^{-1} $M_\odot{}^{-1}$. Given that evolved stellar-populations have [NII]/Hα ratios close to 1 (Belfiore et al. 2016), we subtract $2 \times 1.37 \times 10^{29} \times (M_*/M_\odot)$ erg s^{-1} (corresponding to a sSFR of 1.2×10^{-12} yr^{-1}) from the Hα luminosity to isolate the Hα emission associated with young stars.

Because of the low spectral resolution of the grism, the measured Hα flux contains emission from both Hα and nearby [NII]. To correct for this contamination, we adopt a mass-dependent correction motivated by the mass-metallicity relation. The gas-phase metallicity is estimated from the measured stellar mass assuming the redshift-dependent mass-metallicity relation of Zahid et al. (2014), and the metallicity is converted to a [NII]/Hα flux ratio following Kewley & Ellison (2008). The Hα flux reported in the 3D-HST catalog is reduced by this ratio to determine the Hα flux. This physically-motivated correction (typically around $\sim 25\%$ for our sample) is somewhat larger than the 20% usually assumed (Wuyts et al. 2011).

И тем не менее, модель! Со вспышкой!